Mixed microalgae culture for ammonium removal in the absence of phosphorus: Effect of phosphorus supplementation and process modeling

Ruiz-Martinez, A.*[,a], Serralta, J.[a], Pachés, M.[a], Seco, A.[b], and Ferrer, J.[a]

[a]Instituto de Ingeniería del Agua y Medio Ambiente, IIAMA, Universitat Politècnica de Valencia, Camino de Vera s/n, 46022 Valencia, Spain (e-mail: anruima1@upv.es, jserralt@hma.upv.es, mapacgi@upvnet.upv.es, jferrer@hma.upv.es)

[b]Departament d'Enginyeria Química, Escola Tècnica Superior d'Enginyeria, Universitat de València, Avinguda de la Universitat s/n. 46100 Burjassot, Valencia, Spain (email: aurora.seco@uv.es)

*Corresponding author. Tel. +34 963 877 000 ext. 76176; Fax +34 963 877 618, e-mail address: anruima1@upv.es

ABSTRACT

Microalgal growth and ammonium removal in a P-free medium have been studied in two batch photobioreactors seeded with a mixed microalgal culture and operated for 46 days. A significant amount of ammonium (106 mgN-$NH_4 \cdot l^{-1}$) was removed in a P-free medium, showing that microalgal growth and phosphorus uptake are independent processes. The ammonium removal rate decreased during the experiment, partly due to a decrease in the cellular phosphorus content. After a single phosphate addition in the medium of one of the reactors, intracellular phosphorus content of the corresponding microalgal culture rapidly increased, and so did the ammonium removal rate. These results show how the amount of phosphorus internally stored affects the ammonium removal rate. A mathematical model was proposed to reproduce these observations. The kinetic expression for microalgae growth includes a Monod term and a Hill's function to represent the effect of ammonium and stored polyphosphate concentrations, respectively. The proposed model accurately reproduced the experimental data ($r=0.952$, P-value<0.01).

Keywords

Ammonium removal; microalgae; mathematical modeling; phosphate; wastewater.

HIGHLIGHTS

- Ammonium removal takes place uncoupled from phosphate uptake
- Ammonium removal rate depends on the amount of phosphorus internally stored
- Effect of stored polyphosphate on ammonium removal modelled using Hill's equation
- Enhanced ammonium removal at polyphosphate content higher than 2.2% dry weight

1. INTRODUCTION

Interest on microalgae has increased during the last decades as they constitute a promising alternative for obtaining value-added products and biofuels such as biodiesel, biohydrogen biogas or biocrude. Moreover, microalgal systems for wastewater treatment have long been proposed and studied [1]. These systems range from open-pond cultures to closed photobioreactors [2] and focus primarily on the removal of inorganic nutrients such as ammonium, nitrate and phosphate.

Several studies have proved the suitability of microalgal cultures for nutrient removal in diverse wastewaters. These studies, which showed different degrees of nutrient removal efficiencies, generally agree that the most important advantages of microalgae utilization for this purpose are CO_2 abatement and the possibility of reusing biomass as fertilizer or as renewable source of energy [3-5]. On the other hand, the process spares the otherwise necessary cost of nutrients for algae cultivation. Currently, a rather extended opinion in the scientific community is that the production of algae-based biofuels, at least in the short-term, is neither economically nor energetically feasible without simultaneous wastewater treatment [6].

Phosphorus is an essential component of microalgae. According to the Redfield ratio [7], it constitutes 0.87% of its dry weight. Phosphorus is present in basic cell constituents such as phospholipids, nucleic acids or nucleotides. It can also be accumulated to higher levels inside the microalgal cells, where inorganic polyphosphate serves as reservoir. As reviewed by Powell et al. [8], there are two mechanisms involved in this accumulation: over-compensation, which occurs after re-exposure to phosphorus following a starvation phase, and

luxury uptake, where microalgae accumulate much more phosphorus than it is needed for their survival without previous exposure to P-poor medium.

Different studies, which aimed at defining the polyphosphate accumulation and phosphate uptake dynamics, have shown a relationship between phosphorus stress in the medium and low polyphosphate content in the cells, together with recovery of polyphosphate levels after addition of phosphorus [9-10]. It is also known that starvation enhances the phosphate uptake rate. The effect of P-starvation on ammonium uptake rate is, however, less known. Previous studies did not focus on the influence that polyphosphate content exerts on the nitrogen uptake velocity, as these studies were not undertaken with a wastewater treatment approach.

In the wastewater treatment field mathematical models are useful tools for process design, WWTP scale-up or upgrade, or water quality prediction. Up to now, microalgal growth modelling has been tackled with a diversity of approaches. There are various examples of different complexity-level models which determine phytoplankton evolution in the ecosystems [11-13], content and evolution of intracellular components of interest such as lipids or sugars [14], specific metabolism of single species [15], microalgal production inside photobioreactors [16] or others.

The present work was designed to study the ammonium removal process in a phosphate-free medium and the relationship between the microalgal intracellular phosphorus content and the ammonium removal rate, with a view to designing suitable strategies for wastewater treatment. Therefore it is also the aim of this work to define a kinetic expression for microalgae growth considering the effect of ammonium concentration in the medium and the amount of internally stored polyphosphate on the rate of this process. To this aim, a mathematical model considering microalgae growth and death was proposed and model

parameters were obtained by minimizing differences between experimental data and model predictions. This model should be useful for prediction of ammonium removal rates in wastewater treatment systems.

A microalgal culture was fed only with ammonium in a lab-scale photobioreactor (PBR) and afterwards separated into two identical PBRs. Phosphate was supplied only to one of them. Nutrient uptake kinetics of the two PBRs were studied, as well as biomass composition (%N and %P). Microalgae production-in terms of chemical oxygen demand and suspended solids- was assessed. The experimental data obtained was successfully reproduced by the proposed model. This model can be useful for designing strategies and predicting the behavior of wastewater treatment systems where nutrient removal is achieved by microalgal growth.

2. MATERIALS AND METHODS

2.1. Experimental setup

Three identical PBRs were used in this study (*initial reactor*, *Nitrogen Only Reactor* and *Nitrogen and Phosphorus Reactor*, as it will be explained in section 2.2). Each PBR consisted of a cylindrical, transparent methacrylate tank (20 cm internal diameter) with a total volume of 10 liters (see fig. 1a). The PBRs were closed and the algae culture was mixed by recycling the headspace gas through four fine bubble diffusers mounted at the bottom. Both PBRs were equipped with electronic sensors in order to obtain online measurements of conductivity, oxidation reduction potential, temperature, pH and dissolved oxygen. The probes were connected to a multiparametric analyzer (CONSORT C832, Belgium) and an oximeter (Oxi 320, SET WTW, Germany), respectively. These devices were in turn connected to a PC for data monitoring and storage. Data sampling was conducted every 60 s.

pH in the PBRs was maintained around 7.5 to avoid undesirable processes such as phosphate precipitation and free ammonia stripping. Pure CO_2 (99.9%) from a pressurized cylinder was injected into the gas flow whenever pH exceeded the setpoint of 7.5. Recycling gas from the headspace contributes to minimize the CO_2 requirements for pH control. Since the reactors were closed CO_2 stripping was also minimized but since they were not hermetically sealed extreme overpressure and overaccumulation of oxygen were avoided. Four arrays of 3 vertical fluorescent lamps (Sylvania Grolux, 18 W) 10 cm apart from each other continuously illuminated each PBR from a minimum distance of 10 cm. Photosynthetically active radiation (PAR) of 153 ± 16 μE m^{-2} $s^{-1}$was measured at the surface of the reactors as the arrow in fig. 1b) indicates. The PBRs were placed inside a climatic chamber with air temperature control set to 20 ºC. Due to the constant illumination the temperature in the culture resulted in 25.5 ºC.

A phosphate-free medium, adapted from [17] was used in this study, one litre of which was composed of 115 g $(NH_4)_2SO_4$, 150 mg $CaCO_3$, 400 mg $CaCl_2 \cdot H_2O$, 400 mg $Na_2SeO_3 \cdot 5H_2O$, 350 mg $MgSO_4 \cdot 7H_2O$, 54 mg $(NH_4)_6Mo_7O_2 \cdot 4H_2O$, 30 mg $ZnCl_2$, 30 mg HBO_3, 30 mg $NiCl_2 \cdot 6H_2O$, 18 mg $CuCl_2 \cdot 2H_2O$, 12 mg K_2SO_4, 1.2 mg $FeCl_3 \cdot 4H_2O$, 1.2 mg $CoCl_2 \cdot 6H2O$, 0.6 mg EDTA, 0.3 mg $MnCl_2 \cdot 4H_2O$.

2.2. Operation

7L of a microalgal culture was maintained for 19 days in ammonium-rich and phosphate-free medium in a lab-scale PBR as described in section 2.1, called *initial reactor*. Ammonium in the form of $(NH_4)_2SO_4$ was manually added at the beginning of the experiment and when its concentration dropped below 4 mg NH_4-N·l^{-1} (day 7). On day 19, when ammonium concentration had reached again 4 mg NH_4-N·l^{-1}, the 7 L culture was split into two PBRs,

with a working volume of 3.5 L each. These two PBRs will henceforth be called *NOP* (*Nitrogen Only Reactor)* and *N&PR (Nitrogen and Phosphorus Reactor)* and were not carried out in duplicate. Immediately after the splitting, ammonium in the form of $(NH_4)_2SO_4$ was added into *NOR,* reaching a concentration of 28 mg NH_4-N·l^{-1}, and phosphate in the form of KH_2PO_4 was added into *N&PR,* reaching a concentration of 12 mg PO_4-P·l^{-1}. From then on, both reactors were operated for 27 days. Ammonium was added again in both reactors when its concentration dropped below 4 mg NH_4-N·l^{-1} (day 29 in *NOR* and days 20, 22 and 29 in *N&PR*)

2.3. Microorganisms

The *initial reactor* was seeded with microalgae isolated from the walls of the secondary clarifier in the Carraixet WWTP (Valencia, Spain) and maintained in the laboratory under semi-continuous feeding conditions with a cellular retention time of 4 days and continuous illumination varying between 114 and 198 μE m^{-2} s^{-1}. The effluent of a submerged anaerobic membrane bioreactor (SAnMBR, described in [18]) was used as growth medium. This effluent displays a variable N/P ratio and has been proved to sustain algal growth [5]. Microalgae from the *Chlorococcum* genus together with cyanobacteria (*Spirulina* sp. and *Pseudoanabaena* sp.*)* were identified as the main groups present.

2.4. Analytical Methods

Nutrient removal was evaluated by regular measurements of inorganic nitrogen and phosphorus levels in the samples taken from the PBRs. Ammonium (NH_4-N), nitrite (NO_2-N), nitrate (NO_3-N) and phosphate (PO_4-P) were determined according to Standard Methods [19]

149 (4500-NH3-G, 4500-NO2-B, 4500-NO3-H and 4500-P-F, respectively) in a Smartchem 200
150 automatic analyzer (Westco Scientific Instruments, Westco). Total nitrogen in the algae
151 culture was measured using standard kits (Merck, Darmstadt, Germany, 100613). The acid
152 peroxodisulphate digestion method [19] was used for total phosphorus (TP) measurements.
153 The nitrogen content of the algae biomass was calculated as the difference between total
154 nitrogen and soluble nitrogen. Likewise, the phosphorus content of the algae biomass (total
155 suspended phosphorus, TSP) was calculated as the difference between total phosphorus and
156 orthophosphate concentration. Total and volatile suspended solids (TSS and VSS), as well as
157 chemical oxygen demand (COD) were determined according to Standard Methods [19].

158 All reported results were obtained from the previous analyses conducted in duplicate, except
159 for TSS and VSS where single analysis were made.

160 ## 3. RESULTS AND DISCUSSION

161 ### 3.1. Nutrient removal

162 The composition of the biomass in the *initial reactor* (7 L PBR) after inoculation is included
163 in table 1. According to [20], a phosphorus concentration in the biomass greater than 3%
164 suggests that phosphate luxury uptake has taken place. Therefore, the studied microalgal
165 biomass had stored, before the beginning of this experiment (during the cultivation under
166 semi-continuous mode), more phosphate than needed for growth.

167 Figs. 2a and 2b show the ammonium and phosphate evolution in the *NOR* and *N&PR*,
168 respectively. The experiment started in the 7 L *initial reactor* with biomass inoculation and
169 ammonium addition. The initial VSS and ammonium concentrations were 340 $mgVSS \cdot l^{-1}$ and
170 32 mg $NH_4\text{-}N \cdot l^{-1}$, respectively. Ammonium was added again after 7 days because its

171 concentration was below 4 mg NH_4-N·l^{-1}. During this first period, which is common in both
172 graphs, phosphate concentration in the medium was zero (fig. 2). However, the microalgal
173 biomass removed a total of 58 mg NH_4-N·l^{-1}.

174 Table 1 summarizes the evolution of TSS, VSS and suspended COD in the two reactors
175 during the experiment. Yield coefficients were calculated as the ratio between the amount of
176 biomass generated, measured as VSS and COD, and the ammonium removed.

177 VSS as well as suspended COD concentrations clearly increased in both reactors due to
178 microalgae growth (table 1). This increase was greater in *N&PR* since the amount of
179 ammonium and phosphate taken up was higher.

180 The biomass P content visibly decreased in the *initial reactor* and in the *NOR*, since the
181 microalgae growth took place using the internally stored polyphosphate. In the *N&PR* the
182 biomass P content sharply increased on day 19 (to a maximum of 2.8%) due to phosphorus
183 addition and immediate uptake. It decreased from then on for the rest of the experiment.

184 VSS yield coefficients are similar in the *NOR*, *N&PR* and in the *initial reactor*, whereas the
185 *N&PR* shows a slightly higher COD yield coefficient. It is hypothesized that this difference
186 could be attributed to the amount of phosphate taken up in *N&PR*: growth in *NOR* took place
187 without phosphate addition, like in the *initial reactor*, while in *N&PR* phosphate was
188 available and taken up by microalgae. However, analytical error of the performed
189 measurements (VSS and COD) hinders a clear conclusion on the subject. Biomass N content
190 obtained in the present work is in accordance with the general Redfield formulation [6] of
191 9.20 % (0.092 gN·g^{-1}).

192 **3.1.1. Nitrogen Only Reactor**

As shown in fig. 2a, microalgal ammonium uptake took place during all the experiment (46 days in total) in the *NOR*, without any external phosphate addition. This fact demonstrates that ammonium and phosphorus uptake from the medium are two independent processes-in the sense that one can occur without the other-, and clearly demonstrates that this microalgal culture presents a great capacity for removing a high amount of ammonium in the absence of phosphate in the medium. In this reactor a total of 106 mgN-$NH_4 \cdot l^{-1}$ was removed without phosphate in the culture medium.

After each ammonium addition its uptake took place at a constant rate until ammonium concentration decreased to values around 10-13 mg NH_4-N$\cdot l^{-1}$ (Fig 2a. Filled lines turn into dashed lines). The ammonium uptake rate significantly decreased when ammonium concentrations were below this threshold. This low ammonium affinity observed in these experiments should be taken into account in the design of PBRs for wastewater treatment since large tank volumes or high hydraulic retention times will be required to obtain very low ammonium concentrations. An exception to this was the last slope, when the constant rate was not maintained below 20 mg NH_4-N$\cdot l^{-1}$. This exception will be discussed later in this section. In the *NOR*, the ammonium uptake rate decreased with time throughout the experiment, likely due to a decrease in the internally stored polyphosphate. The selfshading effect of the culture also exerted its influence: biomass growth during the experiment led to a decrease in the available light for microalgae even when the incident light remained constant. The calculated ammonium removal rates (slopes shown in fig. 2a) decreased from 0.209 mgN$\cdot l^{-1} \cdot h^{-1}$ at the beginning of the experiment to 0.09 mgN$\cdot l^{-1} \cdot h^{-1}$ at the end of the experiment. The specific removal rate (mgN$\cdot$mgSSV$^{-1} \cdot h^{-1}$) (table 2) decreased during all the experiment. As no phosphate was added at any time in the *NOR*, the P required for biomass growth could only be taken from their internal P pool, which microalgae had accumulated during the previous phase

of cultivation under semicontinuous conditions. This internal polyphosphate consumption during the experiment led to a decrease in the biomass P content, which reached 0.8% (0.008 $gP \cdot gVSS^{-1}$) at the end of the experiment (at day 46, see table 1), when ammonium removal was taking place at a very slow rate. These results suggest the existence of a relationship between the P content of the cells and the ammonium removal rate. The final biomass P content is a very small value compared to the initial biomass composition (indicated in table 1). It is, according to [20] still higher than the minimum amount of internal phosphorus for cell survival (between 0.2 – 0.4% in dry weight). In fact, [21] has shown a minimum phosphorus content after starvation phase of 0.185 % (0.00185 $gP \cdot g^{-1}$ biomass). However, approaching these minimum values of intracellular P content makes ammonium uptake rate decrease. Around day 35 of the experiment, biomass in the *NOR* reached what seems quite a critical P content. The ammonium uptake rate decreased to very slow values although ammonium concentration was still 20 $mgNH_4\text{-}N \cdot l^{-1}$. At the same time, as table 1 shows, suspended solids significantly increased along the experiment. Mutual shading of the microalgae attenuates light in the PBR and microalgal growth was therefore also slowed down for this reason.

3.1.2. Nitrogen and Phosphorus Reactor

Phosphate was added to *N&PR* on day 19 and reached a concentration of 11.7 mg $PO_4\text{-}P \cdot l^{-1}$. Phosphate removal started immediately and its removal rate was 2 mg $PO_4\text{-}P \cdot l^{-1} \cdot h^{-1}$ until phosphate concentration was nearly zero. This removal rate was very high, considering that while the added phosphate was consumed, only 2.1 mg NH_4-N were taken up by the microalgae. The resulting N:P uptake ratio of 0.18 is very low, which is due to the phosphorus starvation condition of the biomass. The majority of literature values on microalgal phosphate uptake rate under balanced conditions are well below the presented value: [3] reported, for

241 *Chlorococcum*, a value of 0.0475 mg PO_4-P $\cdot l \cdot h^{-1}$ and [22] reported a value of 0.083 mg PO_4-P
242 $\cdot l \cdot h^{-1}$ for *Chlorella* sp. [23] reported for *Chlorella protothecoides* a closer value to the one
243 presented in this work of 1.3 mg PO_4-P$\cdot l^{-1} \cdot h^{-1}$.

244 *N&PR* was spiked with ammonium for a third, fourth and fifth time (fig. 2b). As previously
245 observed in the *NOR*, the ammonium uptake rates kept constant after the ammonium additions
246 but decreased when ammonium concentration in the medium reached values below 10-13 mg
247 NH_4-N$\cdot l^{-1}$. The value obtained for the ammonium removal rate after phosphate addition in the
248 *N&PR* showed a significant increase, due to a fast increase in intracellular phosphorus
249 concentration. Ammonium removal rate decreased along the rest of the experiment, as in
250 *NOR*, due to an increase of selfshading and a decrease in phosphorus content. At the end of
251 the experiment, ammonium concentrations reached lower values in *N&PR* than in *NOR*, and
252 still maintained a faster decreasing trend. At this point, P content of the biomass had reached
253 0.017 gP$\cdot$gVSS^{-1}, which is higher than the biomass P content reached in *NOR* (0.008
254 gP$\cdot$gVSS^{-1}).

255 These results suggest that ammonium removal rate depends on the amount of phosphorus
256 stored in microalgae. Other authors modelled phytoplankton colimitation by nitrogen and
257 phosphorus [24] assuming that the maximum potential for N uptake takes place at high
258 concentrations of intracellular phosphorus, which is in accordance with the experimental
259 results obtained now in this work.

260 The specific ammonium uptake rates (with respect to VSS) obtained in the *N&PR* and the
261 associated biomass P content are shown in table 2, demonstrating how intracellular
262 polyphosphate content exerted a drastic and positive influence in the specific ammonium
263 removal rate: it decreased for the first 2 injections into *initial reactor*, continued decreasing

after the N injections into *NOR* and increased in *N&PR* after P addition, catching up with the initial value of $6x10^{-4}$ mgN·mgSSV^{-1}· h^{-1}. The addition of phosphorus in the medium was the only difference between reactors.

The data shown in table 2 demonstrates therefore a high sensitivity of the specific ammonium removal rate to microalgal P content: the higher the biomass P content the higher the specific ammonium removal rate. However, the relationship between these variables is far from linear: a sharp increase is observed in the specific ammonium removal rate when biomass P content lies between 2.2 and 2.6%. After phosphate addition, the specific ammonium removal rate rose from $2.11x10^{-4}$ for a P content of 2.2% to $6.07x10^{-4}$ mgN·mgSSV^{-1}· h^{-1} for a P content of 2.6%. When biomass P content decreased down to 2.0% due to microalgae growth without phosphate addition the specific ammonium removal rate decreased to a value closed to that previously observed. On the other hand, the selfshading effect due to biomass growth is evidenced by the fact that almost no difference is observed between the ammonium uptake in the *initial reactor* ($6.15x10^{-4}$ mgN·mgSSV^{-1}· h^{-1}) and the *"recovered"* uptake rate in *N&PR* ($6.07x10^{-4}$ mgN·mgSSV^{-1}·h^{-1}) while biomass has quite a different P content (3.7 % and 2.6 % P, respectively) and thus a faster ammonium uptake rate would be expected in *N&PR* if intracellular content was to be the only influencing factor.

Comparison between the performances of both reactors shows that, for this microalgal culture, below the threshold of around 2.2 – 2.6% of internal phosphorus the nitrogen uptake rate decreases considerably and around 1% the microalgal culture is unsuitable for ammonium removal applications due to the slow rate obtained. It has been demonstrated that under phosphorus limitation the nitrogen uptake process takes place at much slower rates. The obtained data also suggest that selfshading influences growth and nutrient uptake rates.

Therefore, these two factors (available light and available intracellular phosphorus content) will be taken into account in the modelling step.

The present work has confirmed, for this microalgal culture, two main consequences of phosphate addition to a P-starving culture:

-Phosphorus supplementation to the medium increases the ammonium removal rate by increasing the amount of polyphosphate the biomass is able to accumulate.

-The added phosphate is removed at a fast rate due to the prior starving conditions. This could be useful in the development of different strategies for wastewater nutrient removal and also shows that biomass growth can still take place with low amounts of phosphorus, as already reported by [25]. These authors proposed a P-starvation cultivation mode to minimize phosphorus resource consumption. A low biomass P content might not be a drawback in some cases, as for instance within a biorefinery concept, where ammonium removal rates are of no concern, or substances of interest are not fertilizers.

3.1.3. Biological nutrient removal

All conclusions drawn from this study are based on the assumption that ammonium and phosphate removal are solely due to microalgal uptake, as the pH control assures that neither free ammonia stripping nor inorganic salts precipitation takes place. Further indication that no inorganic precipitation occurred is the fact that the VSS percentage was always higher than 92% of TSS.

The algal culture studied was mainly composed of three species: *Chlorococcum* sp., *Spirulina* sp. and *Pseudoanabena* sp. A pure culture has not been used in this study as the aim of this

work is to analyze the behavior of the culture which evolved from feeding a PBR with the effluent of a SAnMBR [5]. The results obtained might be applied to those cultures with similar species composition, since the results obtained in a microalga culture composed of close-phylogenetic species with similar nutrient requirements and similar growth conditions might reveal comparable absorption patterns. However, culture from different microalgae clade might show different growth and ammonium removal rates.

On the other hand, the low nitrite and nitrate concentrations measured during all the experiment (highest measured values were 2.2 mg NO_2-N·l^{-1} and 1.7 mg NO_3-N ·l^{-1}) indicate no bacterial nitrification/denitrification activity took place. Constant soluble COD levels (stable around 134 mg COD·l^{-1}) support this hypothesis.

3.2. Mathematical model

3.2.1. Proposed model

A mathematical model focused on the kinetics of microalgal ammonium uptake was proposed with the aim of representing the ammonium removal process observed in the PBRs. The main characteristics of the proposed model are:

- Microalgal ammonium uptake rate does not depend on phosphate concentration in the medium, since ammonium uptake still takes place in a phosphate depleted medium. The rate of this process depends on the amount of phosphate stored. Hill function is proposed to simulate the influence of internal phosphorus concentration on ammonium removal rate since a sharp increase was observed when biomass P content exceeded 2.2%.

- Microalgal ammonium uptake rate depends on ammonium concentration. The Monod kinetics is used to simulate this dependency.

- Biomass is assumed to have a constant composition, excluding the polyphosphate internally stored, which is itself a separate component in the model.

-Phosphate uptake and thus intracellular phosphate accumulation is not considered in the model since this process was not experimentally studied (took place only once when P was supplemented) and thus experimental data is insufficient for obtaining the corresponding kinetic constants. It is considered that the amount of phosphate removed from the medium becomes intracellular polyphosphate. As previously explained, chemical precipitation is avoided with pH control.

-Microalgal death is modelled using a first order kinetics: death rate depends on microalgal concentration. Microalgal death produces inert particulate organic material, with the same N and P composition as the active biomass. No solubilisation processes are considered. The polyphosphate of the dead cells is considered to stay unavailable for further microalgal growth.

-The light influence on the microalgal growth is modelled using the Steele function (1), as suggested by [26] or [27]. A weighted average light intensity, which takes into account the reactor's geometry and the self-shading factor of the microalgae, is used. It is calculated dividing the reactor into discrete concentric sections and applying Lambert-Beer's Law (2) for calculating a uniform light for each section.

$$\frac{I}{k_i}\cdot\exp\left(1-\frac{I}{k_i}\right) \quad (1)$$

$$I = I_0 \cdot \exp(-a \cdot TSS \cdot z) \quad (2)$$

Where I is light intensity ($\mu E \cdot m^{-2} \cdot s^{-1}$), k_i is the optimal light intensity ($\mu E \cdot m^{-2} \cdot s^{-1}$), *a* is the microalgal self-shading factor ($m^2 \cdot gTSS^{-1}$), and *z* (m) is the distance from the surface of the reactor.

The components considered in the model are:

X_{Alg} , microalgal biomass, expressed in $mgCOD \cdot l^{-1}$, excluding internally accumulated polyphosphate.

X_{PP} , intracellular stored polyphosphate, expressed in $mgP \cdot l^{-1}$. It is not included in the mass of X_{Alg} .

X_{Deb} , inert particulate organic material, expressed in $mgCOD \cdot l^{-1}$. Generated in the death process of microalgae, this component accumulated in the reactor during the experiment.

S_{NH4} , ammonium concentration in the medium, expressed in mg NH_4-$N \cdot l^{-1}$.

The kinetic equations proposed for microalgal growth (3) and death (4) are:

$$r = \mu \cdot X_{Alg} \cdot \frac{S_{NH}}{K_S + S_{NH}} \cdot \frac{I}{k_i} \cdot \exp\left(1 - \frac{I}{k_i}\right) \cdot \left(1 - \frac{{k_{XPP}}^n}{{k_{XPP}}^n + \left(X_{PP} / X_{Alg}\right)^n}\right) \quad (3)$$

$$r = b \cdot X_{Alg} \quad (4)$$

The time evolution of all the components can be obtained from the following differential equations:

$$\frac{dX_{Alg}}{dt} = \mu \cdot X_{Alg} \cdot \frac{S_{NH4}}{k_S + S_{NH4}} \cdot \frac{I}{k_i} \cdot \exp\left(1 - \frac{I}{k_i}\right) \cdot \left(1 - \frac{{k_{XPP}}^n}{{k_{XPP}}^n + \left(X_{PP}/X_{Alg}\right)^n}\right) - b \cdot X_{Alg} \quad (5)$$

$$\frac{dS_{NH4}}{dt} = -i_{NAlg} \cdot \mu \cdot X_{Alg} \cdot \frac{S_{NH4}}{k_S + S_{NH4}} \cdot \frac{I}{k_i} \cdot \exp(1 - \frac{I}{k_i}) \cdot \left(1 - \frac{{k_{XPP}}^n}{{k_{XPP}}^n + \left({X_{PP}}/{X_{Alg}}\right)^n}\right) \quad (6)$$

$$\frac{dX_{PP}}{dt} = -i_{PAlg} \cdot \mu \cdot X_{Alg} \cdot \frac{S_{NH4}}{k_S + S_{NH4}} \cdot \frac{I}{k_i} \cdot \exp(1 - \frac{I}{k_i}) \cdot \left(1 - \frac{{k_{XPP}}^n}{{k_{XPP}}^n + \left({X_{PP}}/{X_{Alg}}\right)^n}\right) - b \cdot X_{PP} \quad (7)$$

$$\frac{dX_{Deb}}{dt} = b \cdot X_{Alg} \quad (8)$$

Where i_{PAlg} (gP·gCOD^{-1}) is the phosphorus content of the microalgal structure (constitutional P in X_{Alg}), i_{NAlg} (gN·gCOD^{-1}) is the nitrogen content of the microalgal structure, μ is the maximal growth rate (h^{-1}), K_S represents the halfsaturation constant for ammonium (mgN·l^{-1}), k_{XPP} represents the ratio X_{PP}/X_{Alg} that leads to a 50% reduction of the maximal growth rate (gP·gCOD^{-1}), n is a constant from Hill function, and b is the microalgae death rate (h^{-1}).

3.2.2. Model calibration

Model parameters were determined using the Solver program in Microsoft ® Excel software 2007 for minimizing the residual sum of squared errors between the two sets of experimental data (ammonium concentrations in *N&PR* and *NOR*) and the model predictions.

Initial microalgae, debris, and polyphosphate concentrations are required in order to solve the differential equations. These values can be estimated from suspended COD and TSP measurements (9 and 10) jointly with the steady-state debris balance (11) applied to the reactor where the microalgae were cultivated in semicontinuous mode.

$$susp.COD = X_{Deb} + X_{Alg} \quad (9)$$

$$TSP = X_{PP} + i_{PXAlg} \cdot X_{Alg} \quad (10)$$

$$b \cdot X_{Alg} \cdot \theta = X_{Deb} \quad (11)$$

where θ is the cellular retention time in the semicontinuous reactor where the microalgae used for inoculum were cultivated.

The corresponding boundary conditions were set in the solution procedure every time a reactor was spiked with ammonium. Polyphosphate concentration in *N&PR* was increased according to the observed phosphate decrease during the following 7 hours after the phosphate addition. The initial values for the model parameters were selected based on previous experience and on literature. All concentrations were calculated with a time step of 5 minutes.

i_{NAlg} was established at the initial nitrogen biomass composition (9% gN·gCOD^{-1}) and for i_{PAlg} a value of 0.1% (gP·gCOD^{-1}) was chosen, which is necessarily below the phosphorus total composition of 0.5% (gP·gCOD^{-1}) at the end of the experiment and accounts only for structural phosphorus and not polyphosphate. Figs. 3a and 3b show the model predictions for ammonium concentration and the experimental values along the experiment for *NOR* and *N&PR*, respectively. The obtained parameters, shown in table 3, accurately reproduce the experimental data in both reactors, as shown in fig. 4, where predicted values are plotted against their analytical values with a Pearson correlation coefficient of r = 0.952 (P-value < 0.01, statistical analysis carried out using SPSS 16.1).

For further model validation, a set of data from a shorter but analogous experiment was used. The experiment consisted of an identical reactor where the same procedure as in *N&PR* was followed, with the difference that phosphate was added to the medium after 7 days and the experiment was stopped after 18 days. Moreover, phosphorus was added at a higher concentration of 37 mgP·l^{-1} (fig. 5). Biomass, ammonium and phosphate were characterized as described in section 2.4 in this work. The parameters shown in table 3 were introduced in

410 the model to obtain the corresponding predicted values, which are shown in fig. 5, and also
411 plotted versus their analytical values in fig. 4. The obtained accuracy (r = 0.97, P-value <
412 0.01) confirms the suitability of the model and the determined parameters.

413 One of the most important effects of the higher concentration of added phosphate was that
414 X_{PP}/X_{Alg} ratio reached a maximum of 4% mgP·mgTSS^{-1}. The simulation shows that from day
415 12 of the experiment biomass P content stayed stable around 3% mgP·mgTSS^{-1}, since
416 ammonium was not available for growth. The high internal phosphorus concentration
417 achieved might be the reason why remaining phosphate in the medium was not taken up by
418 the microalgae during this period, as can be seen in fig. 5.

419 The values obtained for μ and k_S are comparable to those obtained by [24]. These authors fit
420 ammonium uptake by *Scenedesmus* sp.LX1 using a Monod equation and obtained values
421 between 0.005 - 0.025 h^{-1} for μ and 4.5 - 13.3 mgN·l^{-1} for K_S. The obtained value for k_{XPP} is in
422 complete accordance with the observations made. Literature k_i values vary in a wide range
423 between 20 and 500 W·m^{-2} ([28] and [26], respectively), in which our 200 µmol·m^2·s^{-1} would
424 be included. The selfshading factor, *a*, also varies in a wide range in literature. Similar values
425 to ours are used in [29-30]. The value obtained in this study for microalgae death rate (*b* =
426 0.002 h^{-1}) compares with literature values ranging from 0.0008 h^{-1} [31] to 0.0058 h^{-1} [32].

427 Measured and predicted COD values are shown in table 4, together with predicted X_{Alg} and
428 X_{Deb}. The predictions of the COD values for initial reactor are in very good accordance with
429 measured values. For *NOR* and *N&PR* the model underestimates COD. Because of the higher
430 mean analytical error in COD measurements, the model has been calibrated to minimize the
431 error in the response for ammonium concentration. The parameters obtained are those which
432 allow the best prediction of ammonium concentration and not of suspended COD values. On

the other hand, the assumption of a constant microalgal N composition (set to its initial measured value of 9%) is a simplification of reality. With a different and/or varying microalgal N content, predicted COD values would have been certainly different. Including a variable microalgae N content according to factors such as N stress, etc., might be the way for improving a model of this kind. This was, however, out of the scope of this paper.

4. CONCLUSIONS

Microalgal growth and ammonium removal in the absence of phosphorus were studied in two mixed cultures of autochthonous microalgae. The results showed that microalgal growth and phosphorus uptake are independent processes. It was also proved that ammonium removal rate depends on the amount of phosphorus internally stored. The proposed microalgal growth model, which includes a Monod term for the effect of ammonium concentration, Hill's function for the effect of the stored polyphosphate concentration and Steele's function for light influence, accurately reproduced the experimental data. Further research should make use of these results for the development of nutrient removal strategies using microalgal cultures.

ACKNOWLEDGEMENTS

This research work has been supported by the Spanish Ministry of Economy and Competitiveness (MINECO, Projects CTM2011-28595-C02-01 and CTM2011-28595-C02-/02) jointly with the European Regional Development Fund (ERDF). They are both gratefully acknowledged.

REFERENCES

[1] Singh, A., Pant, D., Olsen, S.I., Nigam, P.S., 2012. Key issues to consider in microalgae based biodiesel production. Energy Education Science and Technology Part A: Energy Science and Research. 29(1): 563-576

[2] Christenson, L., Sims, R., 2011. Production and harvesting of microalgae for wastewater treatment, biofuels, and bioproducts. Biotechnol. Adv. 29 (6), 686-702.

[3] Aravantinou, A.F., Theodorakopoulos, M.A., Manariotis, I.D., 2013. Selection of microalgae for wastewater treatment and potential lipids production. Bioresour. Technol. 147, 130-134.

[4] Arbib, Z., Ruiz, J., Álvarez-Diaz, P., Garrido-Pérez, C., Perales, J. A., 2014. Capability of different microalgae species for phytoremediation processes: wastewater tertiary treatment, CO_2 bio-fixation and low cost biofuels production. Water Res 49, 465-474.

[5] Ruiz-Martinez, A., Martin Garcia, N., Romero, I., Seco, A., Ferrer, J., 2012. Microalgae cultivation in wastewater: Nutrient removal from anaerobic membrane bioreactor effluent. Bioresour. Technol. 126, 247-253.

[6] Pittman, J. K., Dean, A. P. 2011. The potential of sustainable algal biofuel production using wastewater resources. Bioresour. Technol. 102, 17-25.

[7] Redfield, A., 1958. The biological control of chemical factors in the environment. Am. Sci. 46, 205-221.

[8] Powell, N., Shilton, A., Chisti, Y., Pratt, S., 2009. Towards a luxury uptake process via microalgae – Defining the polyphosphate dynamics. Water Research 43, 4207-4213.

478 [9] Jansson, M., 1993. Uptake, exchange, and excretion of orthophosphate in
479 phosphate-starved *Scenedesmus quadricauda* and *Pseudomonas* K7. Limnol.
480 Oceanogr. 38(6), 1162-1178.
481 [10] Nishikawa, K., Machida, H., Yamakoshi, Y., Ohtomo, R., Saito, K., Tominaga,
482 N., 2006. Polyphosphate metabolism in an acidophilic alga *Chlamydomonas*
483 *acidophila* KT-1 (Chlorophyta) under phosphate stress. Plant Sci. 170, 307-313.
484 [11] Geider, R.J., MacIntiyre, H.L., Kana, T.M., 1997. Dynamic model of
485 phytoplankton growth and acclimation: responses of the balanced growth rate and the
486 chlorophyll *a*:carbon ratio to light, nutrient-limitation and temperature. Mar. Ecol.
487 Prog. Ser. 148, 187-200.
488 [12] Geider. R.J., MacIntiyre, H.L., Kana, T.M., 1998. A dynamic regulatory model
489 of phytoplanktonic acclimation to light, nutrients, and temperature. Limnol.
490 Oceanogr., 43(4), 679-694.
491 [13] Reichert, P., Borchardt, D., Henze, M., Rauch, W., Shanahan, P., Somlyódy,
492 L., Vanrolleghem, P., 2000. River Water Quality Model No. 1. International Water
493 Association, London.
494 [14] Mairet, F., Bernard, O., Masci, P., Lacour, T., Sciandra, A., 2011. Modelling
495 neutral lipid production by the microalga *Isochrysis* aff. *galbana* under nitrogen
496 limitation. Bioresour. Technol. 102, 142-149.
497 [15] Kliphuis, A.M.J., Klok, A.J., Martens, D.E., Lamers, P.P, Janssen, M.,
498 Wijffels, R.H., 2011. Metabolic modeling of *Chlamydomonas reinhardtii*: energy
499 requirements for photoautotrophic growth and maintenance. J. Appl. Phycol. 24(2),
500 253-266.

501 [16] Fernández, I., García-Acién, F.G., Fernández, J.M., Guzmán, J.L., Magán, J.J.,
502 Berenguel, M., 2012. Dynamic model of microalgal production in tubular
503 photobioreactors. Bioresour. Technol. 126, 172-181.
504 [17] Li, J., Ozgun, H., Ersahin, M. 2011. Procedure of SMA test. Section of
505 Sanitary Engineering, Delft University of Technology.
506
507 [18] Giménez, J.B., Robles, A., Carretero, L., Durán, F., Ruano, M.V., Gatti, M.N.,
508 Ribes, J., Ferrer, J., Seco, A., 2011. Experimental study of the anaerobic urban
509 wastewater treatment in a submerged hollow-fibre membrane bioreactor at pilot scale.
510 Bioresour. Technol. 102, 8799-8806.
511 [19] APHA, A., WEF, 2005. Standard Methods for the Examination of Waters and
512 Wastewaters. 21st ed. Washington DC.
513 [20] Reynolds, C.S., 2006. The Ecology of Phytoplankton (Ecology, Biodiversity
514 and Conservation). Cambridge University Press, Cambridge, UK.
515 [21] Markou, G., 2012. Alteration of the biomass composition of *Arthrospira*
516 *(Spirulina) platensis* under various amounts of limited phosphorus. Bioresour.
517 Technol. 116, 533-535.
518 [22] Aslan, S., Kapdan, I.K., 2006. Batch kinetics of nitrogen and phosphorus
519 removal from synthetic wastewater by algae. Ecol. Eng. 28, 64-70.
520 [23] Ramos Tercero, E.A., Sforza, E., Morandini, M., Bertucco, A. 2014.
521 Cultivation of *Chlorella protothecoides* with urban wastewater in continuous
522 photobioreactor: Biomass productivity and nutrient removal. Appl Biochem
523 Biotechnol 172, 1470–1485

[24] Bougaran, G., Bernard, O., Sciandra, A., 2010. Modeling continuous cultures of microalgae colimited by nitrogen and phosphorus. J. Theor. Biol. 265, 443-454.

[25] Wu, Y.H., Yu, Y., Hu, H.Y., Potential biomass yield per phosphorus and lipid accumulation property of seven microalgal species, 2013a. Bioresour. Technol. 130, 599-602.

[26] Reichert, P., Borchardt, D., Henze, M., Rauch, W., Shanahan, P., Somlyódy, L., Vanrolleghem, P., 2001. River Water Quality Model no. 1 (RWQM1):II. Biochemical process equations. Water Sci. Technol .43 (5) 11-30.

[27] Wu, Y.H., Li, X., Yu, Y., Hu, H.Y., Zhang, T.Y., Li, F.M., 2013b. An integrated microalgal growth model and its application to optimize the biomass production of *Scenedesmus* sp. LX1 in open pond under the nutrient level of domestic secondary effluent. Bioresour. Technol. 144, 445-451.

[28] Broekhuizen, N., Park, J. B. K., McBride, G. B., Craggs, R. J., 2012. Modification, calibration and verification of the IWA River Water Quality Model to simulate a pilot-scale high rate algal pond. Water Res. 46 (9) 2911-2926.

[29] Quinn, J., de Winter, L., Bradley, T., 2011. Microalgae bulk growth model with application to industrial scale systems. Bioresour. Technol. 102, 5083–5092.

[30] Ketheesan, B., Nirmalakhandan, N., 2013. Modeling microalgal growth in an airlift-driven raceway reactor. Bioresour. Technol. 136, 689–696.

[31] Barbosa, M.J., Hadiyanto, H., Wijffels, R.H., 2004. Overcoming shear stress of microalgae cultures in sparged photobioreactors. Biotechnol. Bioeng. 85(1), 78-85.

[32] Centeno da Rosa, A.P., Fernandes Carvalho, L., Goldbeck, L., Vieira Costa, J.A., 2011. Carbon dioxide fixation by microalgae cultivated in open bioreactors. Energy Convers. Manag. 52, 3071–3073.

548 **FIGURE LEGENDS**

549 Fig. 1: a) Experimental setup; b) illumination and measuring point.

550 Fig. 2: Ammonium and phosphate evolution in a) *NOR* and b) *N&PR* during the whole
551 experiment.

552 Fig. 3: Time evolution of ammonium concentration in a) *NOR* and b) *N&PR*, along with
553 model predictions.

554 Fig. 4: Predicted values plotted against their corresponding analytical values. Empty dots
555 correspond to this experiment for model calibration and full dots correspond to data from
556 previous experiment for model validation.

557 Fig. 5: Time evolution of ammonium and phosphate concentrations in the model validation
558 dataset, along with model predictions.

559

560 **TABLES**

561

562 Table 1: Biomass evolution in the reactors and calculated yields.

Time (d)	TSS[a] ($mg \cdot l^{-1}$)	VSS[a] ($mg \cdot l^{-1}$)	Susp COD[b] ($mg \cdot l^{-1}$)	Biomass N content ($gN \cdot gVSS^{-1}$)	Biomass P content ($gP \cdot gVSS^{-1}$)	Yield coefficient $Y_{N\text{-}VSS}$ ($gVSS \cdot gN^{-1}$)	Yield coefficie $Y_{N\text{-}COD}$ ($gCOD \cdot gN^{-1}$)
0	380	340	517	11.8%	3.7%	--	--
19 (end of *initial reactor*)	882	817	1176	12.0%	1.6%	8.2	11.3
46 (end of *NOR*)	1330	1224	1880	10.8%	0.8%	8.8	12.8
46 (end of *N&PR*)	1583	1460	2320	10.6%	1.7%	8.7	13.9

563 Mean analytical error: [a] 50 $mg \cdot l^{-1}$; [b] 70 $mg \cdot l^{-1}$;

564

565

566 Table 2: Calculated net and specific ammonium removal rate after each ammonium addition

567 in each reactor, together with biomass P content at those moments (beginning of slope).

Reactor	Slope number	Removal rate ($mgN \cdot l^{-1} \cdot h^{-1}$)	Slope error	Specific removal rate ($mgN \cdot mgVSS^{-1} \cdot h^{-1}$)	Biomass P content ($gP \cdot gVSS^{-1}$)
initial	1	0.209	0.018	$6.15x10^{-4}$	3.7%
	2	0.121	0.002	$2.11x10^{-4}$	2.2%
N	3	0.152	0.001	$1.86x10^{-4}$	1.6%
	4	0.090	0.009	$8.79x10^{-5}$	1.0%
P	3	0.514	0.051	$6.07x10^{-4}$	2.6%
	4	0.247	0.004	$2.41x10^{-4}$	2.0%
	5	0.176	0.014	$1.41x10^{-4}$	1.5%

568

569

570 Table 3: Obtained parameters

Parameter	Units	Obtained value
μ	h^{-1}	0.042
k_S	$mgN \cdot l^{-1}$	12
n	-	1.35
K_{XPP}	$mgP \cdot mgCOD^{-1}$	0.027
k_I	$\mu E \cdot m^2 \cdot s^{-1}$	200
b	h^{-1}	0.0005
a	$m^2 \cdot gTSS^{-1}$	0.03

571

572

573 Table 4: Measured COD values. Predicted total COD, X_{Alg} and X_{Deb} values.

Time (d)	Measured Susp COD ($mg \cdot l^{-1}$)	Predicted Susp COD ($mg \cdot l^{-1}$)	X_{Alg} ($gCOD \cdot l^{-1}$)	X_{Deb} ($gCOD \cdot l^{-1}$)
0 (inoculum)	517	517	434	83
19 (end of *initial reactor*)	1176	1132	535	596
46 (end of *NOR*)	1880	1554	357	1196
46 (end of *N&PR*)	2320	1624	412	1212

574

575

576 **FIGURES**

577

578 **Fig. 1**

579

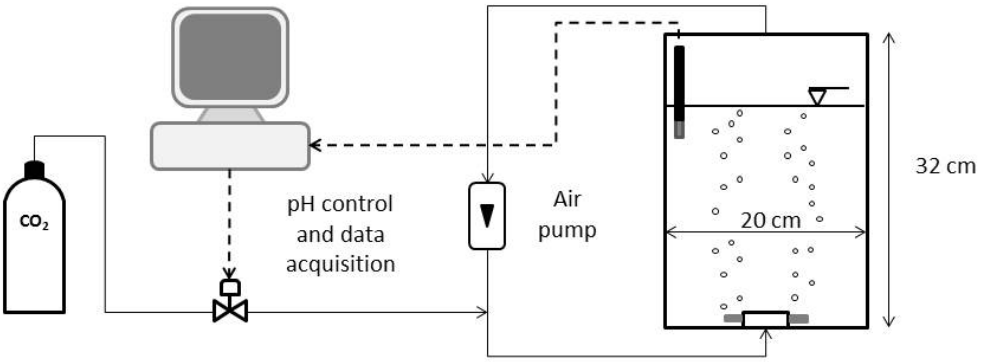

a)

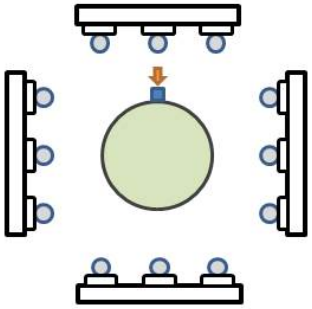

b)

580

581

582 **Fig. 2**

583

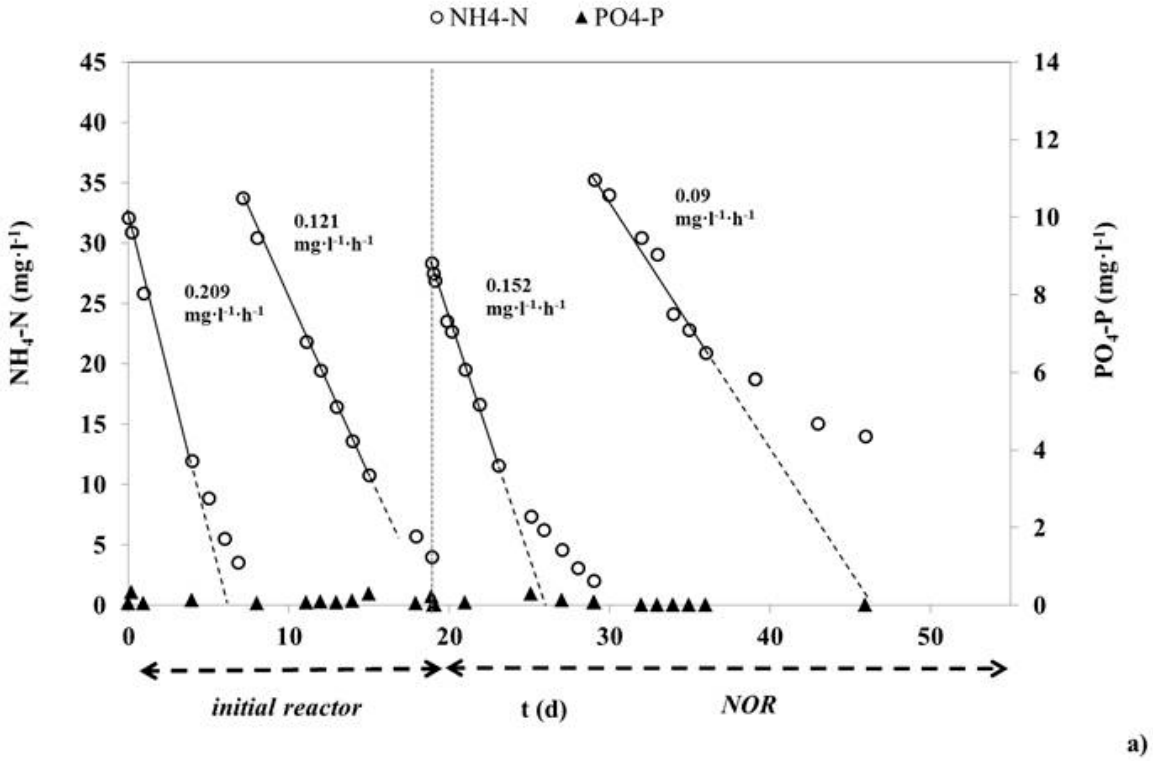

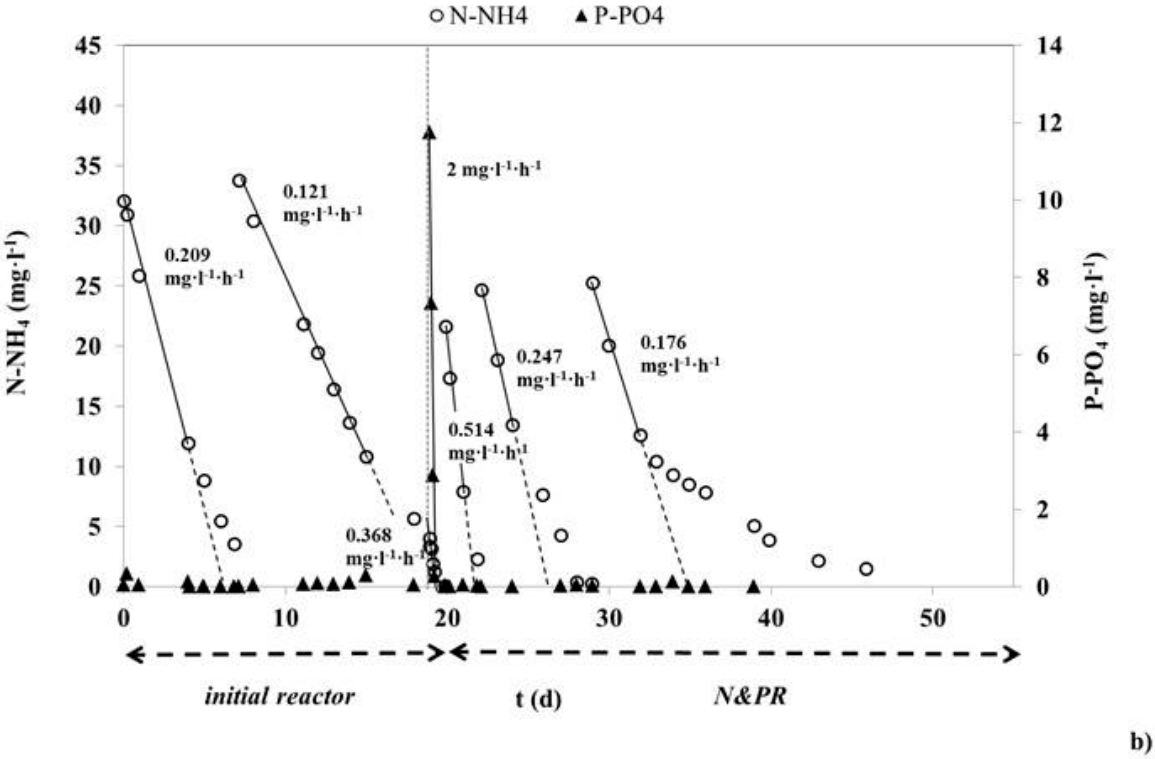

584

585 **Fig. 3**

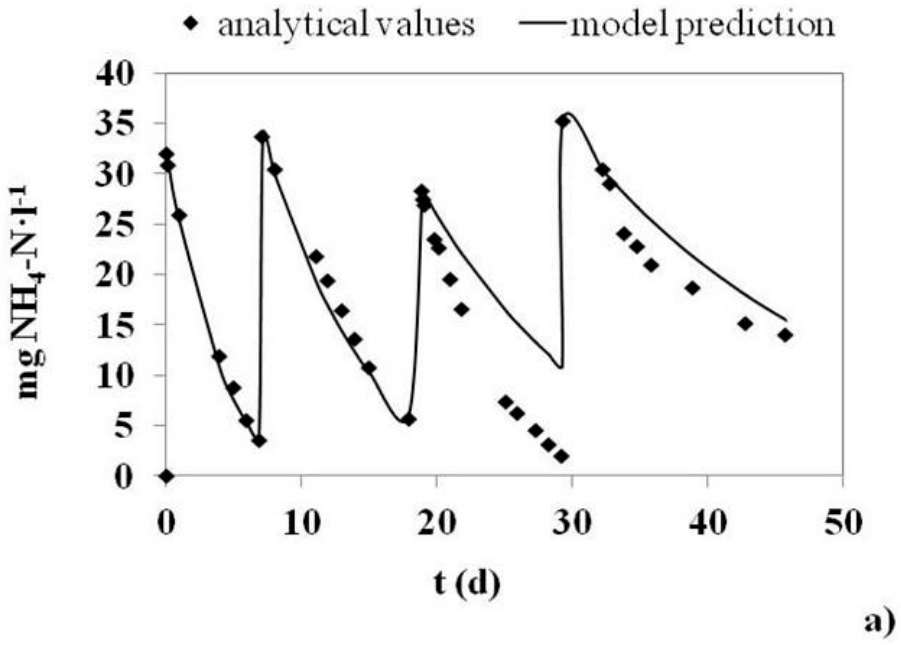

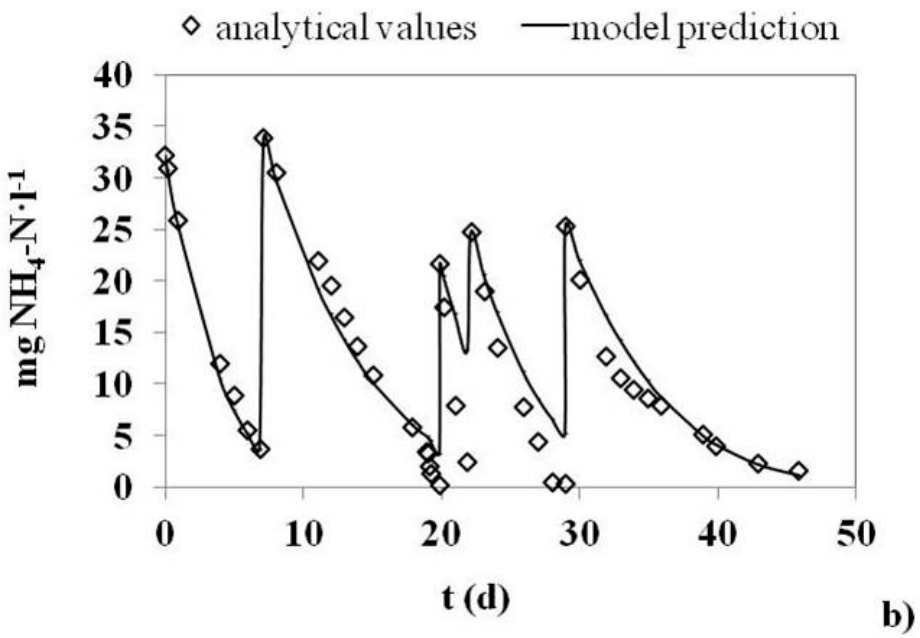

586

587

588

589 **Fig. 4**

590

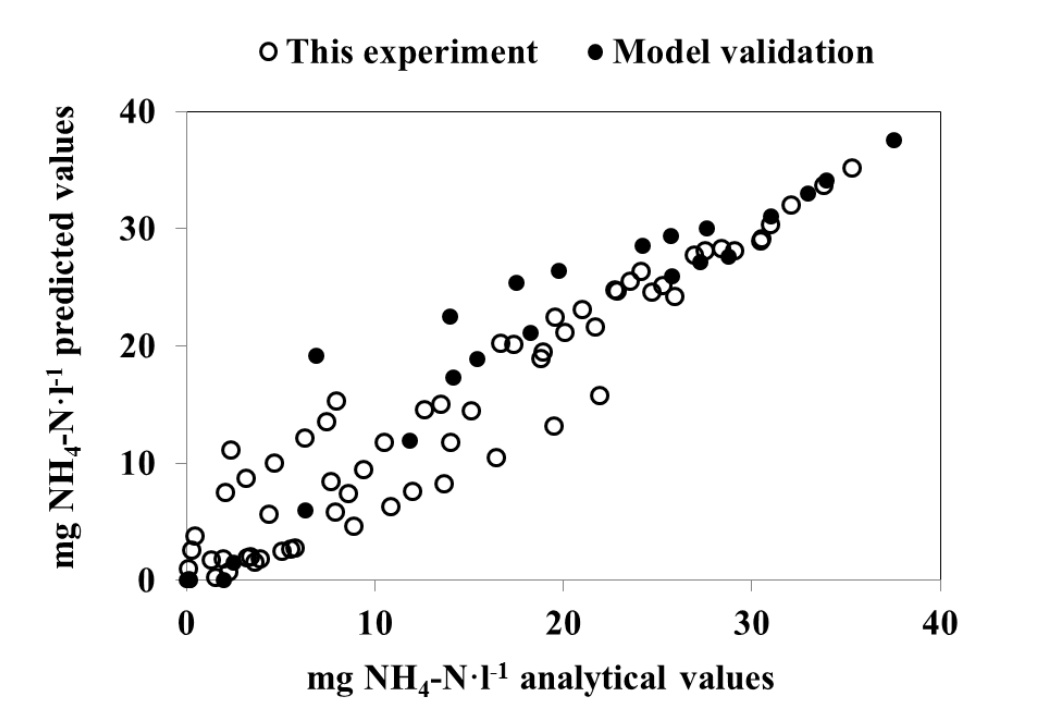

591

592

593 **Fig. 5**

594

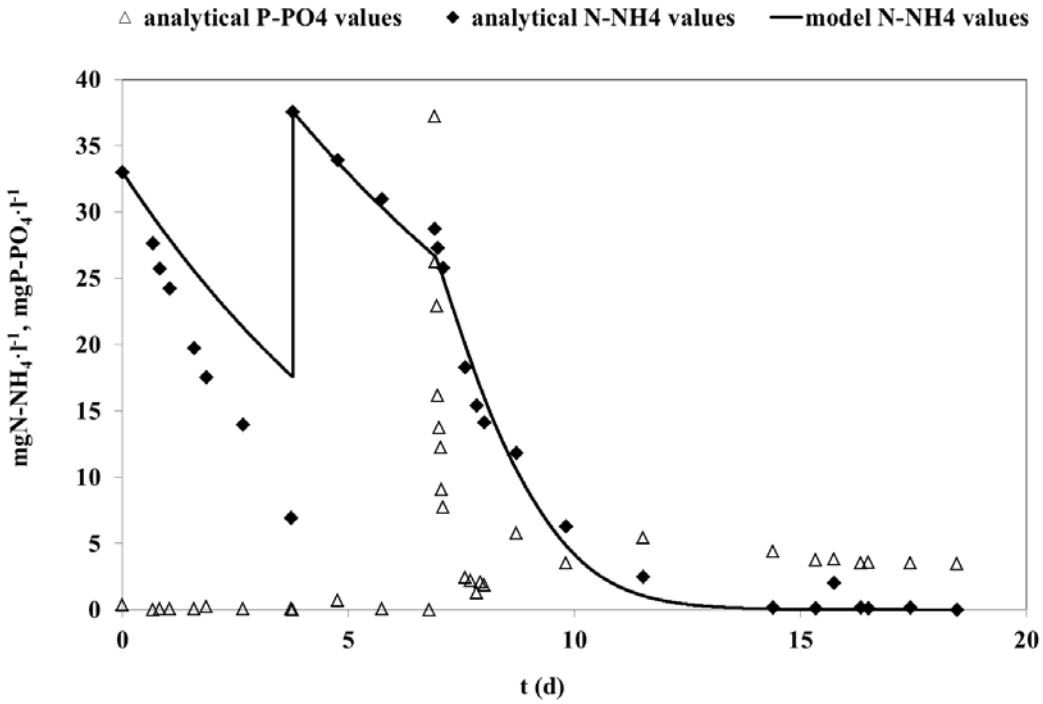

595